Thin Solid Films 518 (2010) 6334–6338

Contents lists available at ScienceDirect

Thin Solid Films

journal homepage: www.elsevier.com/locate/tsf

Uniformity of gallium doped zinc oxide thin film prepared by pulsed laser deposition

Fumiaki Mitsugi*, Yoshihiro Umeda, Norihiro Sakai, Tomoaki Ikegami

Graduate School of Science and Technology, Kumamoto University, 2-39-1 Kurokami, Kumamoto 860-8555, Japan

ARTICLE INFO

Available online 24 March 2010

Keywords:
Transparent conducting oxide
Amorphous gallium doped zinc oxide
Pulsed laser deposition
Room temperature deposition
Large-area deposition

ABSTRACT

Recently, transparent conducting oxide thin films have attracted attention for the application to transparent conducting electrodes. In this work, we evaluated the uniformity of electrical, optical and structural properties for gallium doped zinc oxide thin films prepared on the 10×10 cm^2 silica glass substrate by pulsed laser deposition. The resistivity, carrier concentration, mobility, bonding state and atomic composition of the film were uniform along in-plane and depth direction over the 10×10 cm^2 area of the substrate. The film showed the average transmittance of 81–87%, resistivity of 1.4×10^{-3} Ω cm, carrier concentration of 9.7×10^{20}/cm^3 and mobility of 5 cm^2/Vs in spite of the amorphous X-ray diffraction pattern. The gradual thickness distribution was found, however, the potential for large-area and low temperature deposition of transparent conducting oxide thin film using pulsed laser deposition method was confirmed.

1. Introduction

The demand of transparent conducting oxide (TCO) thin films has been increasing for applications such as flat panel displays, solar cells and functional windows. Although the indium tin oxide (ITO) thin film has been used in commercial products as transparent electrodes, research for an alternative material and its thin film deposition technique is required because of the high cost of indium and its limited supply. In recent years, zinc oxide (ZnO) doped with group-III elements has shown promising properties as an inexpensive and alternative TCO material. Doped ZnO thin films have been prepared using several methods such as sputtering [1–3], sol–gel [4,5], vacuum arc plasma evaporation [6] and pulsed laser deposition (PLD) [7–11]. In many cases, thin films are heated during deposition [2,7–11] or post-annealed after deposition [3–5] because most of all researchers focus on crystallized doped ZnO thin films with c-axis orientation. We have also evaluated characteristics of crystallized Al-doped ZnO and Ga-doped ZnO (GZO) thin films prepared at the substrate temperature of 100–500 °C by PLD in previous works [12–14]. However, recently, techniques for low temperature (below 150 °C) deposition are desired to deposit films on plastic substrates such as polyethylene-terephtalate (PET) and polyethylene-naphtalate (PEN) for flexible device application. Then, we have put our attention to doped ZnO thin films deposited by PLD at room temperature, which have relatively comparable electrical and optical characteristics to those of crystallized thin films [15]. The concept of amorphous transparent semiconductors was firstly proposed by Hosono et al. [16–18] and amorphous TCO thin films have been researched recently [19–21]. We have attempted to prepare doped ZnO thin films with good properties on relatively large substrates using PLD at room temperature though it has been recognized that PLD is not a suitable method for large-area deposition in spite of its features of low temperature deposition and good stoichiometric controllability. There are several reports on large-area deposition techniques for doped ZnO thin films. The typical technique is a magnetron sputtering method using dual-cathodes which is called in-line sputtering [22,23]. Shirakata et al. reported a reactive plasma deposition technique using two plasma guns with a traveling substrate system [24]. In general, these methods use several plasma sources and a one-dimensional substrate scanning system. On the other hand, PLD method for large-area deposition uses a two-dimensional substrate scanning or a laser scanning system because a uniform deposition area is too small for the size of commercial scale substrate and they make the PLD system more complex and expensive. In this paper, we report uniformity of electrical, optical and structural properties of the GZO thin film deposited on 10×10 cm^2 silica glass substrate set at 28 cm apart from the target as well as target–substrate distance dependency.

2. Experimental setup

A KrF excimer laser (Lambda Physik Compex205, maximum energy = 650 mJ) was introduced into a stainless chamber through a mirror, a lens, and a quartz glass window. Finally, it was focused on a GZO target ($\Phi = 3$ cm, 5 wt.% $Ga_2O_3 \pm 95$ wt.% ZnO) with the incident angle of 45°, the laser energy density of 2 J/cm^2 (laser energy = 200 mJ) and repetition rate of 10 Hz. A 10×10 cm^2 silica glass substrate was placed on a substrate holder which was faced to the target and had neither a heater nor a scanning system. Masking tapes (0.3 cm width) were put on the substrate to make an undeposited area for a film thickness measurement. The distance between the

* Corresponding author. Tel./fax: +81 96 342 3572.
E-mail address: mitsugi@cs.kumamoto-u.acjp (F. Mitsugi).

0040-6090/$ – see front matter © 2010 Elsevier B.V. All rights reserved.
doi:10.1016/j.tsf.2010.03.044

target and the substrate was 28 cm. The target–substrate distance effect was studied by varying the distance from 4.5 cm to 28 cm. The chamber was evacuated to a base pressure of 10^{-3} Pa by a turbo pump and then the deposition was carried out at the pressure. The deposition time of 30 min and 45 min was used to prepare two GZO thin films of different thickness. After the deposition, the substrate was cut into 7 square pieces along the diagonal line for the evaluation of the film uniformity. Properties of the film were evaluated using the following methods. The film thickness was observed by cross-sectional analysis of atomic force microscopy (AFM: SII, SPM3800N). The optical transmittance was measured using a UV−VIS light source (Ocean Optics, DT-MINI) and a multichannel spectrometer (Ocean Optics, HR4000, 200–1100 nm). The sheet resistance (R_S) was measured by conventional four-point probe technique. The carrier concentration (n), mobility (μ_H), and resistivity (ρ_H) were determined by Hall measurement using the van der Pauw configuration in the magnetic field of 0.28 T. Structural characterization was confirmed using an X-ray diffractometer (XRD: Rigaku, RINT2000) with CuKα radiation. X-ray photoelectron spectroscopy (XPS: VG Scientific, Sigma Probe) with AlKα (1486.6 eV) was used to study the binding state of films. Its spatial resolution on the sample surface and the energy resolution were 400 μm and 0.1 eV, respectively. An Ar ion etching gun (VGEX05) was used for the depth profile measurement.

3. Results and discussions

At first, we investigated the target–substrate distance (d) dependency of the film thickness (t) and electric properties of the GZO thin film deposited at room temperature in vacuum (10^{-3} Pa). In conventional use of PLD, a substrate is placed at a position near the target where plasma plume covers the substrate. We have already reported on in-plane uniformity of GZO thin films prepared at the d of 4.5 cm where the substrate was exposed in the plasma plume [15]. Fig. 1 shows relationship of t versus d^{-2} for GZO thin films deposited for 30 min. It is revealed that the relationship can be followed by $t \propto d^{-2}$ except for the deposition at $d = 4.5$ cm which means the ablated species propagate with keeping conic section from the ablation point due to the long mean free path of the species in vacuum. This relationship is well agreed with that in case of vacuum evaporation. It is assumed that the deposition area is proportional approximately to d^2 because the ablated species can not diffuse due to their high kinetic energy. The relatively thicker thickness at $d = 4.5$ cm which is out of the relationship of $t \propto d^{-2}$ may be affected by species with higher energy in plasma plume.

Fig. 2 shows the d dependence of ρ_H, n and μ_H for GZO thin films measured by the Hall measurement. As can be seen in Fig. 2, the n is almost independent on the d. The average n is 1.3×10^{21}/cm^3. The μ_H value for the film deposited at $d = 4.5$ cm where the film is exposed by the plasma plume is remarkably lower and which results in the increase of the ρ_H. The μ_H decreases and the ρ_H that is inversely proportional to the μ_H increases gradually with the increase of the d except for the $d = 4.5$ cm. However, it can be expressed that the change of the μ_H and the ρ_H is very little, nevertheless the d is changed in the long range. The collision less propagation of the ablated species may contribute to this result. The μ_H and the ρ_H range from 6.8 to 8.8 cm^2/Vs and from 5.0×10^{-4} to 9.2×10^{-4} Ω cm, respectively. The relatively high μ_H of the not crystallized film may be caused by the overlapping s-orbit between neighboring Zn or Ga. These values are slightly inferior to those of crystallized GZO thin films however these results indicate that the film deposited at room temperature has the potential as the transparent electrode from the electrical point of view.

Then, we investigated the in-plane uniformity of the GZO thin film deposited at $d = 28$ cm on 10×10 cm^2 silica glass substrate. Fig. 3 shows the film thickness distributions for the GZO thin films deposited at $d = 28$ cm for 30 min and 45 min. The abscissa means the measurement position along the diagonal line of the GZO thin film deposited on the 10×10 cm^2 substrate. The position of 0 cm corresponds to the center of the GZO thin film. The AFM images of the edge of the film at each position were observed in the range of 20×20 μm^2 area. The thickness in Fig. 3 indicates the average value in the area with a ±5% uncertainty due to the surface roughness of the thin film. The distribution of the film thickness is symmetrical with respect to the center point. The deposition rate estimated from Fig. 3, is 2.3 nm/min (3.8×10^{-3} nm/pulse) at the center of the film. This deposition rate seems low for PLD, however the deposition area is quite large compared to the conventional PLD configuration where a target–substrate distance is of the order of several cm. The film thickness at the position of 5.4 cm is approximately 72% compared to that at the center. This relatively gentle thickness distribution was caused by the long mean free path of ablated species in vacuum pressure of 10^{-3} Pa. The inset figure shows the XRD spectrum of the film deposited for 45 min at the center position. The crystallization peaks were not observed. The reason may be the less migration

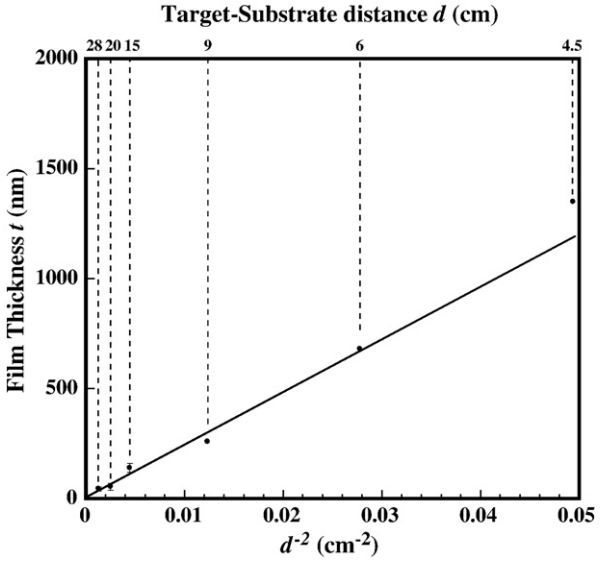

Fig. 1. The relationship between film thickness (t) and target–substrate distance (d) for GZO thin films deposited for 30 min.

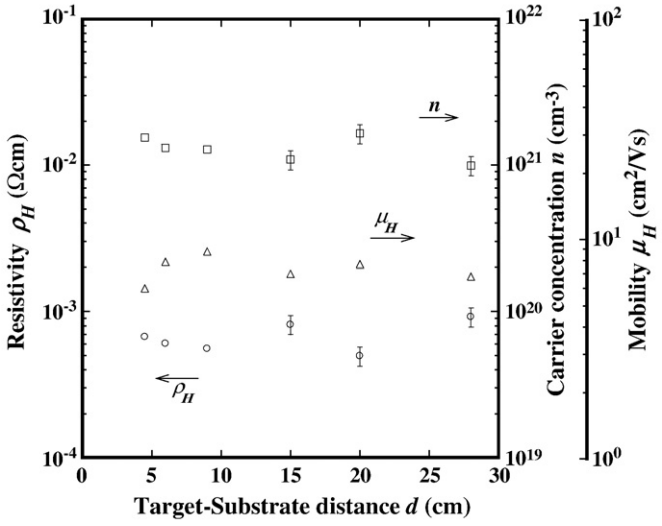

Fig. 2. The target–substrate distance (d) dependence of the resistivity (ρ_H), carrier concentration (n) and mobility (μ_H) for the GZO thin films measured by the Hall measurement using the van der Pauw configuration.

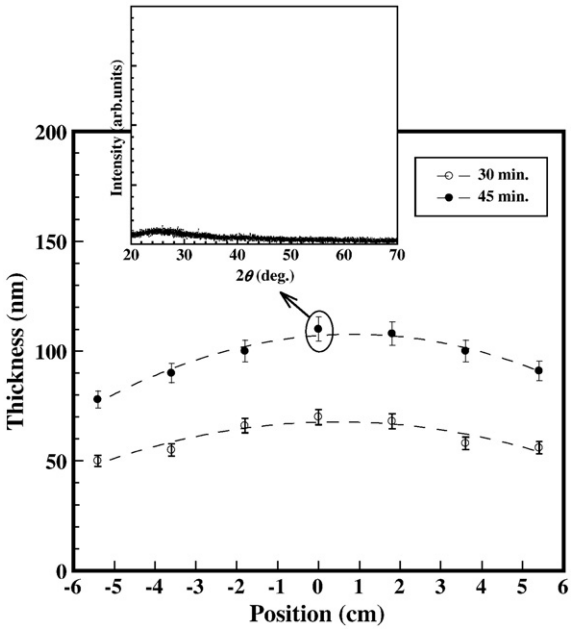

Fig. 3. The film thickness distribution of the GZO thin films deposited at target–substrate distance (d) of 28 cm for 30 min and 45 min. The position indicates the distance from the film center. The inset shows the XRD spectrum for the film deposited for 45 min at the center position.

energy of species on the substrate. It is understandable the gentle thickness distribution in case of the deposition at the target–substrate distance of 28 cm but it is difficult to expect that the film properties such as the resistivity and the atomic composition are uniform over such large-area film since it is recognized that film property strongly depends on the deposition position or plasma region in PLD method. Then, we investigated the position dependency of the optical transmittance, the electrical properties, the binding state and the atomic composition on the depositing position of the GZO thin film. The typical transmittance properties of GZO thin films deposited for 45 min are shown in Fig. 4. The inset figure shows the extinction coefficient k of the films calculated from the transmittance curves. The average transmittance in 400–800 nm wavelength range at the positions 0 cm, 1.8 cm, 3.6 cm and 5.4 cm for 45 min deposited films are 81%, 83%, 85% and 86%, respectively. These transmittance values are comparable with those of commercial TCO thin films. The transmittance increases when the measurement position is apart from the center. This transmittance change attributes to the film thickness because the extinction coefficient of the film is independent on the position as can be seen in the inset figure. Fig. 5 shows sheet resistance R_S and resistivity (ρ_S) distribution for the GZO thin films measured by the four-point probe technique. The measurement was carried out using currents of 0.1, 0.5 and 1.0 mA in air at room temperature. In this figure, R_S means the averaged value and a correction factor of 4.0095 was taken into consideration. The ρ_S was calculated using the R_S and the thickness shown in Fig. 3 for comparison with ρ_H measured by the van der Pauw configuration. Here, the error bar of the film thickness was neglected. As can be seen in this figure, the ρ_S depends on neither the film thickness nor the position and the average ρ_S is 1.5×10^{-3} Ω cm. Therefore, it is found that the R_S is inversely proportional to the film thickness. In other words, it is possible to control R_S of the GZO thin film by adjusting only the film thickness with taking into account its transmittance. The position dependency of ρ_H, n and μ_H measured by the van der Pauw configuration is shown in Fig. 6. As is evident from Fig. 6, the ρ_H, n and μ_H of the film deposited for 30 min are almost the same as those of the film deposited for 45 min. In addition, it is also noted that the ρ_H, n and μ_H have little position dependency. The average ρ_H, n and μ_H estimated from the two films (14 samples) are 1.4×10^{-3} Ω cm, 9.7×10^{20}/cm^3 and 5 cm^2/Vs, respectively. It is confirmed that there is a good agreement of the average values between ρ_H and ρ_S. The ρ_H is relatively low though the film is prepared at room temperature in vacuum, but a few times higher than those of crystallized GZO films which have been reported [6,24]. The ρ_H is inversely proportional to the μ_H. The μ_H value of 5 cm^2/Vs is relatively lower than that of the crystallized GZO film. We assume that the relatively low μ_H is ascribable to the amorphous structure of the film where the degree of overlapping between neighboring 4s electron orbits of Zn or Ga may be lower compared to that of the crystallized film due to the structural disorder. However, the μ_H value of our GZO film is larger than that of amorphous semiconductor such as a-Si:H (<1 cm^2/Vs). It is known as Drude's theory that the optical reflection occurs in the visible region when the n is greater than about 2×10^{21}/cm^3. The plasma resonance wavelength estimated from the Drude's theory using the n of 9.7×10^{20}/cm^3 and μ_H of 5 cm^2/Vs was approximately 1700 nm, that

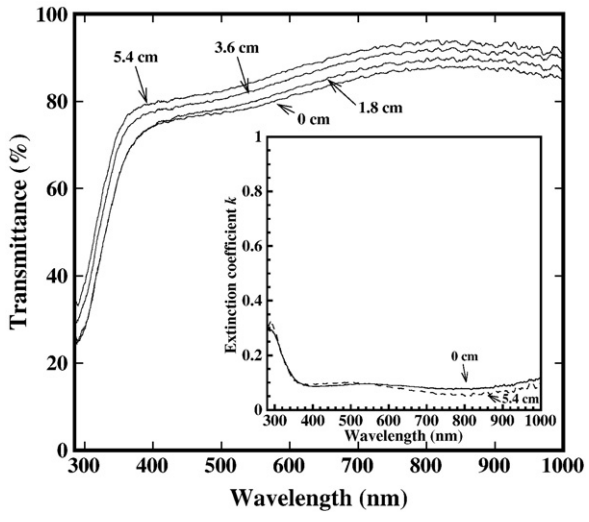

Fig. 4. The transmittance property of the GZO thin films deposited for 45 min. The inset figure shows the extinction coefficient versus the wavelength property.

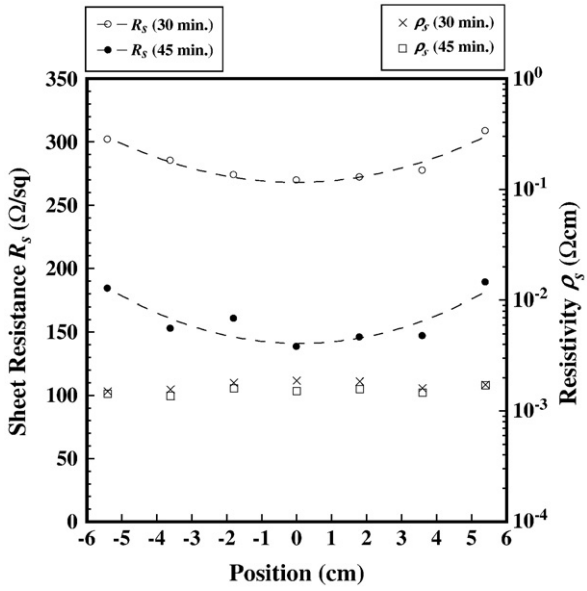

Fig. 5. The position dependence of the sheet resistance (R_S) and the resistivity (ρ_S) for the GZO thin films deposited for 30 min and 45 min measured by the four-point probe technique.

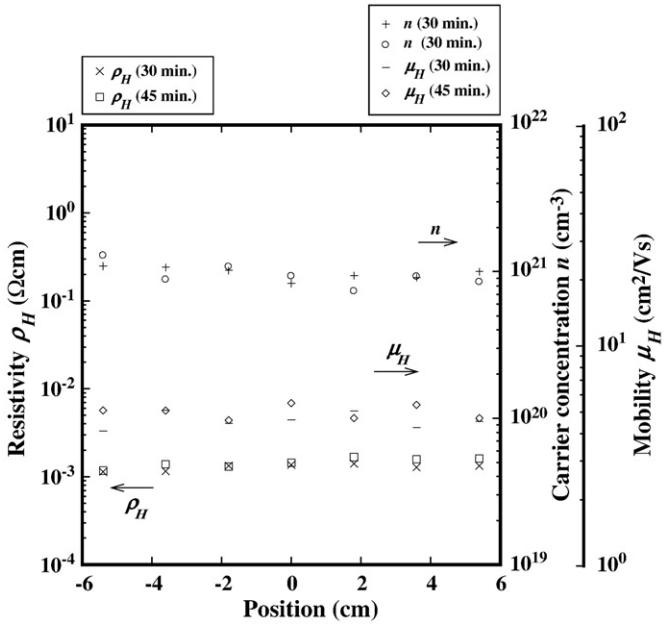

Fig. 6. The position dependence of the resistivity (ρ_H), carrier concentration (n) and mobility (μ_H) for the GZO thin films deposited for 30 min and 45 min obtained by the Hall measurement using the van der Pauw configuration.

is the reason why the decrease of the transmittance can not be seen at a longer wavelength region in Fig. 4.

XPS depth profiles were measured for each sample to investigate the position dependency of the chemical state and the atomic composition. As a result, we could observe similar depth profiles at each position. Therefore, we report typical XPS depth profiles on Ga2p, Zn2p and O1s for one sample (position = 0 cm) of the film deposited for 30 min. Fig. 7 shows the XPS depth profiles on Ga2p taken at the different depths by etching the film using Ar ion for 1 min after each scan. The film was etched completely and the substrate appeared after 10 min etching then the calculated etching rate was approximately 7 nm/min. It is evident from Fig. 7 that the position and the intensity of the Ga2p peak do not change from the surface of the film to the interface with the substrate. This means that Ga is doped constantly along the depth direction of the film. The binding energies of 1118.5 eV for $Ga2p_{3/2}$ and 1145.4 eV for $Ga2p_{1/2}$, indicated with broken lines in Fig. 7, shift by 1.4 eV higher than binding energies of

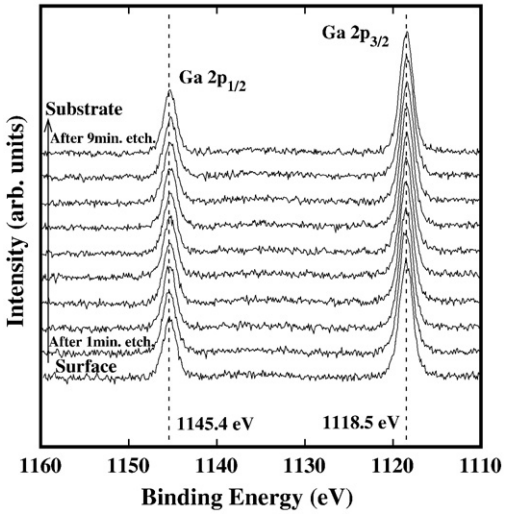

Fig. 7. The XPS depth profile on Ga2p of the GZO thin film (position = 0 cm) deposited for 30 min.

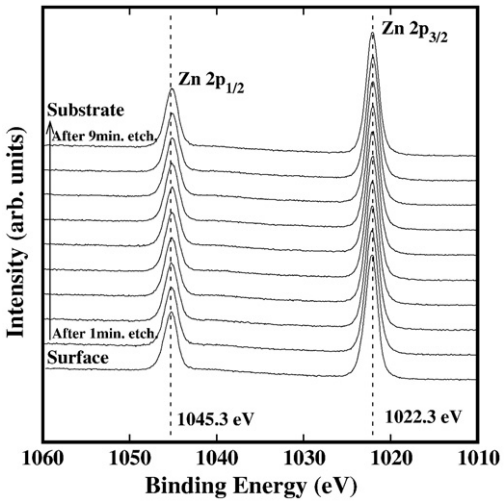

Fig. 8. The XPS depth profile on Zn2p of the GZO thin film (position = 0 cm) deposited for 30 min.

Ga metal. This phenomenon is a striking evidence of the binding between Ga and O in the film. Fig. 8 shows the XPS depth profile on Zn2p for the sample. It is found that the composition and the bonding state of Zn do not change along the depth direction. The binding energies of 1022.3 eV for $Zn2p_{3/2}$ and 1045.3 eV for $Zn2p_{1/2}$ shift by 0.3 eV higher than those of Zn metal due to the binding between the Zn and O. Fig. 9 is the XPS depth profile on O1s for the sample. It should be pointed out that O1s peak, especially at the film surface, is composed from two Gaussian peaks of peak I (530.9 eV) and peak II (532.5 eV) as described in Fig. 9. Peak I originated from the oxygen binding with Ga and Zn because it shows the slightly lower binding energy compared to the theoretical value (531.0 eV) and remains after 9 min etching. On the other hand, the intensity of peak II decreased with the increase of the etching. Since the O/Zn ratio was greater than 1 when peak II was included in the atomic composition calculation, we consider that peak II may arise from absorbed oxygen or vapor in the film. The atomic composition of the GZO thin film along the depth direction was deduced using the $Ga2p_{3/2}$, $Zn2p_{3/2}$ and O1s peaks. As for the O1s peak, we used only peak I for the estimation. The average atomic composition of the GZO thin film was Ga:Zn:O = 0.04:0.52:0.44. The atomic composition was almost constant along the depth direction. An additional important finding here is that

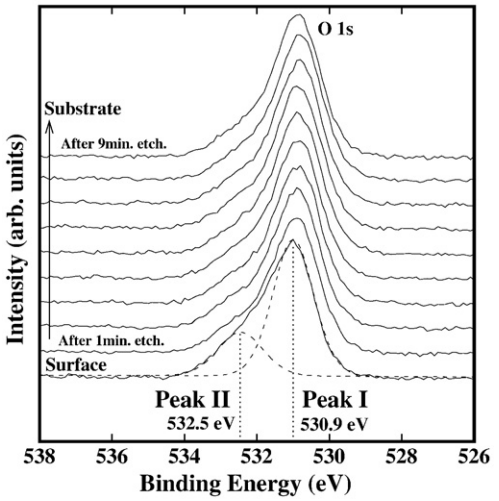

Fig. 9. The XPS depth profile on O1s of the GZO thin film (position = 0 cm) deposited for 30 min. The dashed curves are a result of Gaussian peak fitting.

the oxygen vacancy occurs but it is relatively suppressed in spite of the deposition in vacuum. Consequently, not only the Ga doping but also the moderate oxygen vacancy increased the electron carrier density of the GZO film up to $9.7\times10^{20}/cm^3$, which resulted in relatively good conductivity. It is assumed that the ablated species lose little their kinetic energy at the substrate position of 28 cm from the target due to the collision less propagation in vacuum and the GZO thin film which has relatively close composition to the target can be deposited. The film is not able to be crystallized at room temperature but the crystallization is not necessary in the case of this material because the electron mobility can be obtained via the s-orbit of Zn and Ga.

4. Conclusions

From above mentioned results, it was found that the ρ_H (ρ_S), n, μ_H, light absorption coefficient, bonding state and atomic composition of the GZO thin film were uniform along in-plane and depth direction within the 10×10 cm^2 area. The transmittance and the R_S were varied with the quite gentle thickness distribution due to the long distance of 28 cm between the substrate and the target. In this study, GZO thin film deposition using the longer target–substrate distance over 28 cm could not be conducted due to the structural limitation of our equipment, however, it seems possible to obtain larger GZO thin films with keeping the uniformity of the ρ_H (ρ_S), n, μ_H, absorption coefficient, bonding state and atomic composition by extending the target–substrate distance.

Acknowledgement

The authors would like to express their thanks to Professor Y. Nakamura of the Kumamoto University for valuable advice and technical support.

References

[1] P. Singh, A.K. Chawla, D. Kaur, R. Chandra, Mater. Lett. 61 (2007) 2050.
[2] S. Mandal, R.K. Singha, A. Dhar, S.K. Ray, Mater. Res. Bull. 43 (2008) 244.
[3] W. Lin, R. Ma, W. Shao, B. Liu, Appl. Surf. Sci. 253 (2007) 5179.
[4] S. Bandyopadhyay, G.K. Paul, S.K. Sen, Sol. Energy Mater. Sol. Cells 71 (2002) 103.
[5] G.K. Paul, S.K. Sen, Mater. Lett. 57 (2002) 959.
[6] T. Minami, S. Ida, T. Miyata, Y. Minamino, Thin Solid Films 445 (2003) 268.
[7] B.-Z. Dong, G.-J. Fang, J.-F. Wang, W.-J. Guan, X.-Z. Zhao, J. Appl. Phys. 101 (2007) 033713.
[8] V. Bhosle, A. Tiwari, J. Narayan, Appl. Phys. Lett. 88 (2006) 032106.
[9] J.N. Zeng, J.K. Low, Z.M. Ren, T. Liew, Y.F. Lu, Appl. Surf. Sci. 197–198 (2002) 362.
[10] H. Agura, Y. Takase, K. Uehara, A. Nakamura, Y. Higashimura, T. Aoki, A. Suzuki, T. Matsushita, M. Okuda, H. Okinaka, IEE J. Trans. Electron. Inf. Syst. 126 (11) (2006) 1268 [in Japanese].
[11] F.K. Shan, G.X. Liu, W.J. Lee, G.H. Lee, I.S. kim, B.C. Shin, Y.C. Kim, J. Cryst. Growth 277 (2005) 284.
[12] S.-M. Park, T. Ikegami, K. Ebihara, Jpn. J. Appl. Phys. 44 (2005) 8027.
[13] S.-M. Park, T. Ikegami, K. Ebihara, Thin Solid Films 513 (2006) 90.
[14] S.-M. Park, T. Ikegami, K. Ebihara, P.-K. Shin, Appl. Surf. Sci. 253 (2006) 1522.
[15] N. Sakai, Y. Umeda, F. Mitsugi, and T. Ikegami: to be published in Surf. Coat. Technol.
[16] H. Hosono, N. Kikuchi, N. Ueda, H. Kawazoe, K. Shimidzu, Appl. Phys. Lett. 67 (1995) 2663.
[17] H. Hosono, Y. Yamashita, N. Ueda, H. Kawazoe, K. Shimidzu, Appl. Phys. Lett. 68 (1996) 661.
[18] H. Hosono, Thin Solid Films 515 (2007) 6000.
[19] J.M. Khoshman, M.E. Kordesch, Thin Solid Films 515 (2007) 7393.
[20] C.W. Ow-Yang, H.-Y. Yeom, D.C. Paine, Thin Solid Films 516 (2008) 3105.
[21] D. Kang, I. Song, C. Kim, Y. Park, T.D. Kang, H.S. Lee, J.-W. Park, S.H. Baek, S.-H. Choi, H. Lee, Appl. Phys. Lett. 91 (2007) 091910.
[22] B. Szyszka, V. Sittinger, X. Jiang, R.J. Hong, W. Werner, A. Pflug, M. Ruske, A. Lopp, Thin Solid Films 442 (2003) 179.
[23] S. Calnan, J. Hupkes, B. Rech, H. Siekmann, A.N. Tiwari, Thin Solid Films 516 (2008) 1242.
[24] S. Shirakata, T. Sakemi, K. Awai, T. Yamamoto, Superlattices Microstruct. 39 (2006) 218.